

Upgrading the shear strength of non-ductile reinforced concrete frame connections using FRP overlay systems

Mohamad J. Terro

Associate Professor. Civil Engineering Department, Kuwait University.

Sameer Hamoush

Associate Professor. Architectural Engineering Department, North Carolina AandT State University.

Moetaz El-Hawary

Research Scientist, Building and Energy Tech. Dept., Kuwait Institute for Scientific Research, PO Box 24885 Safat 13109, Kuwait. Email: mhawary@safat.kisr.edu.kw

ABSTRACT: This investigation presents the use of Fiber Reinforced Polymer (FRP) composite systems in upgrading existing reinforced concrete frames to meet strength and ductility requirements laid out in recent ACI building codes (ACI-318. 2002). Analytical calculations are presented for the shear behavior of frames strengthened with layers of FRP and an experimental study is carried out to verify the mechanical properties of the proposed FRP systems with various fiber architecture designs. Carbon and fiber glass FRP systems have been analysed. Flat layers and corrugated shapes with rectangular and circular configurations are employed in the retrofitting systems in addition to various orientations of the fibers which are taken into consideration. The ductility requirement is ensured by controlling the out of plane flexural rigidity of the FRP systems. The desired out of plane rigidity is obtained by increasing the thickness of the FRP systems or by corrugating the applied FRP overlays. In conclusion, this study has shown that the use of FRP systems is an efficient and viable repair method for upgrading concrete frame connections with shear deficiency.

KEYWORDS: shear; FRP; connections; strength; ductility

1 INTRODUCTION

Rehabilitation of non-ductile concrete frame joints to improve strength, confinement, and ductility has gained considerable attention in recent years (Scott 1996, Hwang and Lee 1999, 2000). Most investigations in the literature aimed at the study of the behaviour of the RC frame connections and their rehabilitation to meet recent design considerations or provide adequate shear reinforcement after exposure to seismic loads. A repair method using epoxy injection, removal and replacement of crushed concrete, and RC jacketing of heavily damaged joints according to the United Nations Industrial Development Organization (UNIDO) manual guidelines has been proposed, Tsonos (1999). The use of corrugated steel jacketing has also been suggested and evaluated to upgrade RC frame connections, Bidda *et al.* (1997). Strengthening RC T-joints with Carbon FRP systems have been investigated experimentally, Gergely *et al.* (2000). Design aids for such joints have been developed in that study. The orientation of the fibres and the surface preparation were found to affect the efficiency and level of shear strengthening of the joints.

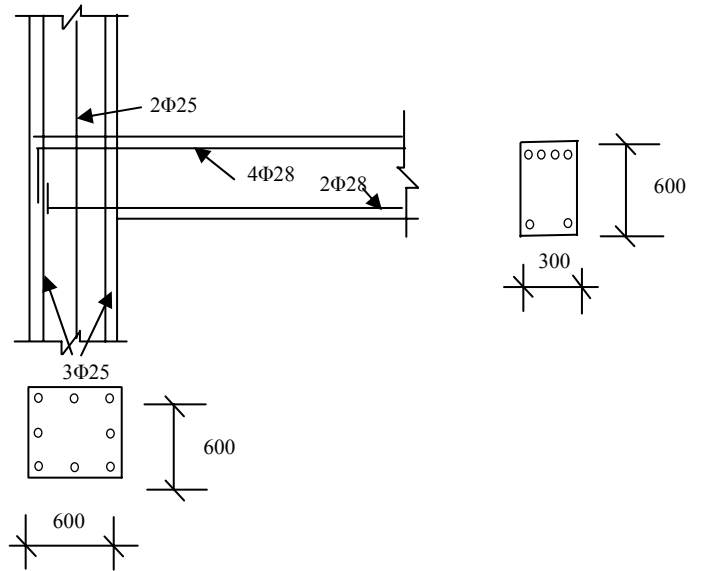
The study, Gergely *et al.* (2000), demonstrated the viability and efficiency of the use of carbon FRP systems in improving the shear capacity of T-joints. The analytical and design models used for selecting the FRP repair systems for improving shear strength, however, is still the *subject* of research and requires significant refinement to ensure optimal repair designs and system performance.

In this paper, the analysis of rehabilitation systems using glass and carbon FRP layers to upgrade the shear strength in deficient concrete frame connections is discussed. The upgrading techniques are aimed at the strength and ductility requirements laid out in recent ACI building codes, ACI (2002). An experimental work is carried out including rectangular and circular corrugated shapes in the retrofitting systems with different orientations of the fibres. The out of plane flexural rigidity of the FRP systems ensures the ductility requirement whereas strength requirements are met by increasing the thickness and/or corrugating the applied FRP overlays.

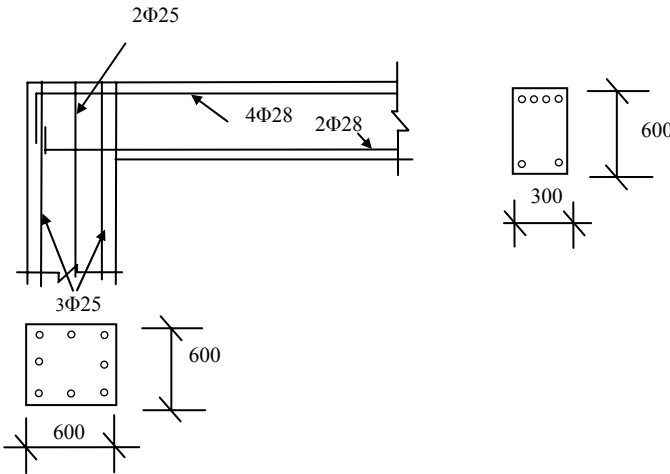
2 SPECIMEN DESIGN

A frame connection is considered in the design of equivalent FRP retrofitting systems for upgrading connections with deficiency in shear. The frame connection is shown in Figure 1(a, b, c and d) in typical connection with and without spandrel beams for one and three story structures. The cross section of the beam is 300 x 600 mm with 2 Φ 28 (2 bars of diameter 28 mm) bottom reinforcement and 4 Φ 28 for the top steel. The column has a cross section of 600 x 600 mm with 8 Φ 25 reinforcement. Cover to reinforcement of 40 mm was maintained for all members. The utilized mix consists of 330 kg of ordinary Portland cement, 640 kg of crushed sand and 1280 kg of quartzite coarse aggregates with water to cement ratio of 0.5.

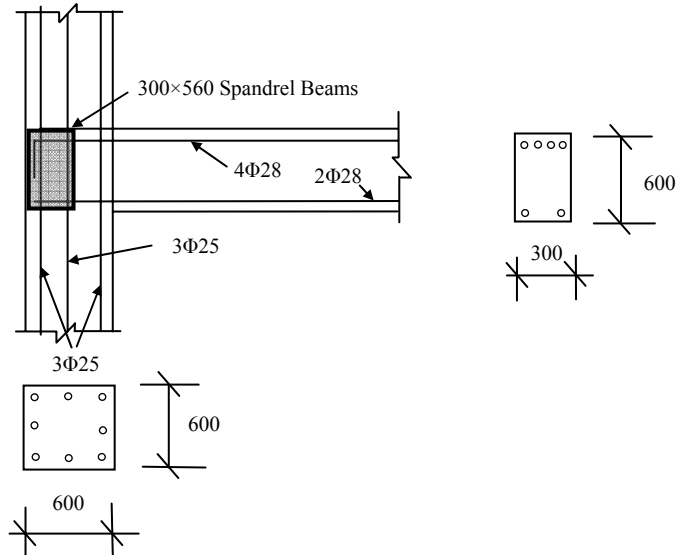
The compressive strength of concrete (f_c') is 27.6 MPa, and the steel yield stress (f_y) 413.7 MPa.



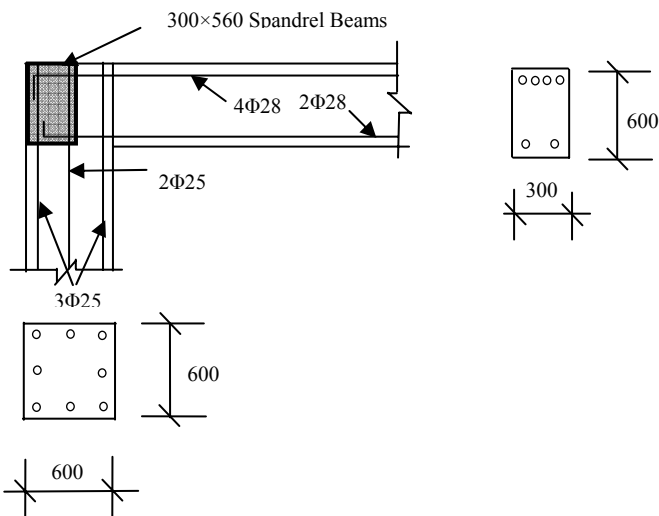
(c) Typical exterior connection without spandrel beams for a three-story structure (dimensions in mm).



(a) Typical exterior connection without spandrel beams for a one-story structure (dimensions in mm).



(d) Typical exterior connection with spandrel beams for a three-story structure (dimensions in mm).



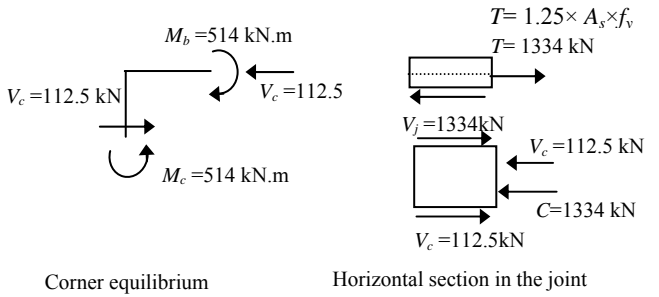
(b) Typical exterior connection with spandrel beams for a one-story structure (dimensions in mm).

Figure 1. Typical connection designs considered in the analysis of FRP repair systems.

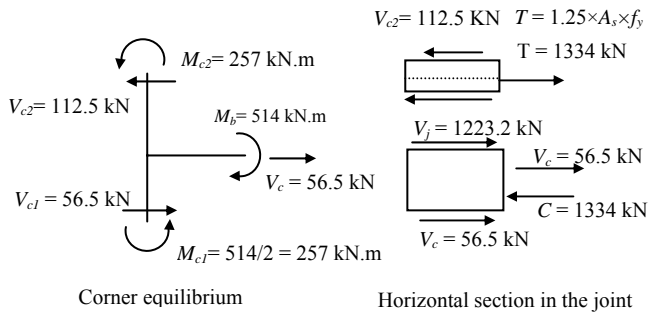
3 SHEAR DESIGN BASED ON ACI-318 (2002)

The calculated ultimate moment capacity of the beam forming the joint is 514 kN.m.

Figures 2 (a) and (b) show free body diagrams of the joints in figures 1 (a) and (c) respectively. A 4.5 m length is considered for columns



(a) Free body diagram for the joint in Figure 1 (a).



(b) Free body diagram for joint in Figure 1 (c).

Figure 2. Free body diagrams for typical exterior joints.

3.1 Shear Calculation of the Joint

The nominal shear strength of the connection is given in ACI 318-02 code as:

$$V_n = \gamma(f'_c)^{1/2} b_j h \quad (1)$$

Where V_n is the nominal shear stress, γ is the fracture of unbalanced moment, b_j is the average dimension and h is the overall thickness.

For the joints in Figure 1, γ is 1, b_j is $\frac{1}{2}(300+600) = 450$ mm, and h is 600 mm.

$$V_n = 1(27.6)^{1/2} 450 \times 600 / 1000 = 1418.5 \text{ kN} \geq V_j = 1334.4 \text{ kN} \quad (2)$$

where, V_j is the factored shear force and $h = 600 \geq 20 \times b_d = 20 \times (31.75) = 571.5$ mm.

Therefore, the dimension of the joint is acceptable.

3.2 Design of the Required Transverse Steel

The required steel area is derived as follows:

$$A_{sh} \geq 0.3 \times s_h \times h_c \times \left(\frac{f'_c}{f_{yh}} \right) \times \left(\frac{A_g}{A_c} - 1 \right) \quad (3)$$

But, not less than:

$$A_{sh} \geq 0.09 \times s_h \times h_c \times \left(\frac{f'_c}{f_{yh}} \right) \quad (4)$$

Where, A_{sh} is total cross-sectional area, s_h is the spacing of transverse reinforcement, h_c is the cross-sectional dimension of column core, A_g is the gross area, A_c is the cross-sectional area of the structural member and f_{yh} is the specified yield strength of shear reinforcement.

$$h_c = 600 - 2 \times (38 + 12.0 / 2) = 511 \text{ mm.}$$

where, 38 mm is the concrete cover and 12 mm is the stirrup diameter.

$$A_c = (600 - 2 \times 38)^2 = 275000 \text{ mm}^2 \quad (5)$$

$$\frac{A_{sh}}{S_h} = 0.3 \times 511 \times (27.6 / 413.7) \times ((600 \times 600 / 275000) - 1) = 3.16 \text{ mm} \quad (6)$$

$$\frac{A_{sh}}{S_h} = 0.09 \times 511 \times (27.6 / 413.7) = 3.07 \text{ mm} \quad (7)$$

Therefore, the value for $\frac{A_{sh}}{S_h}$ in equation (6) controls.

Spacing of the hoops s_x is the minimum of:

$\frac{1}{4}$ of the minimum member dimension

$$(0.25 \times 600 = 150 \text{ mm})$$

six times the smallest longitudinal beams bars diameter ($6 \times 28.6 = 171.5 \text{ mm}$)

s_x as defined by:

$$s_x = 100 + (350 - h_x) / 3$$

Where,

$$h_x = 300 - 38 - 12.7 / 2 = 255.7 \text{ mm}$$

$$\therefore s_x = 100 + (350 - 255.7) / 3 = 131.5 \text{ mm}$$

150 mm, and not less than 100 mm.

Based on the above, s_x is chosen as 100 mm.

$$A_{sh} = 100 \times 3.16 = 316 \text{ mm}^2$$

Use hoops of 12mm diameter with three legs in each direction ($A_{sh} = 339 \text{ mm}^2$) as shown in Figure 3.

It can be noted that the amount of reinforcement for joint of Figure 1 (b) is the same as that for joint of Figure 1(a), since the spandrel beam does not cover $\frac{3}{4}$ of the joint surface area. The spandrel beam cross section is $300 \times 560 = 168000 \text{ mm}^2$. The joint surface area is 360000 mm^2 .

If a larger section for the spandrel beam is used, the transverse steel requirement will be cut to half of the calculated value above. The spacing between the hoops will be limited to 150 mm.

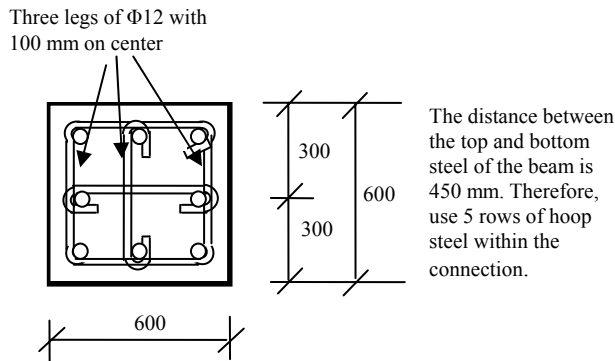


Figure 3: Steel reinforcement in the cross section of the connection (Dimensions in mm).

4 SHEAR CONNECTIONS REINFORCED WITH FRP SYSTEMS

In this section, the design is based on the strength requirements as specified by the hoop steel area provided by the ACI 318-02 Code and the ductility requirements as specified by the hoop steel spacing.

4.1 Strength Requirements

Simple analytical procedures are developed to design the retrofitting system to satisfy the strength requirements of concrete connections using the ACI-318-02 Code recommendations. The analysis is based on the assumption that an equivalent force generated by the FRP materials ($f_{ul} \times s \times t_f$) replaces the required confining force exerted by the hoop steel ($A_{sh} \times f_y$). The equivalent force in the FRP materials is calculated at a stress level (F_{ul}/SF), where the F_{ul} is the rupture stress of the FRP materials, and SF is the safety factor assumed to have a value of 2.

The required thickness of the FRP materials over the s (spacing between the hoop steel) is given by simple mechanics as

$$t_f = 2 \times A_{sh} \times f_y / (f_{ul} \times s) \quad (8)$$

Where, t_f is the thickness of the FRP materials.

To calculate the equivalent cross sectional area of the FRP materials for various fibre architectures, an experimental program was performed to evaluate the axial and flexural engineering properties of various FRP fibre architectures. In the testing program, eight configurations were tested in axial tension (ASTM

D-3039-00) and the remaining eight configurations in flexural bending (ASTM D-790-92). The evaluated configurations consisted of two fibre materials, carbon and glass, and two lay-ups of the fibre orientations. The fibre orientations were limited to $0/90^\circ$ and $\pm 45^\circ$.

The material properties of the fibers used in the experimental program are shown in Table 1.

The resin used was ATLAC 580-05 Vinyl Ester in room temperature curing. Summary of the experimental program is shown in Tables 2 (a) and (b). The fiber balance

Table 1. Properties of the fiber used

Composite Materials	Glass BFG 2532	Carbon W-5-322
Ultimate Tension Strength (MPa)	345	483
Ultimate Elongation	1.25 %	1.0 %
Elastic Modulus (GPa)	27.6	48.3
Design Thickness (mm/layer)	0.2718	0.3302

was maintained for all specimens of the experimental program. Also, it must be mentioned that the thickness of the bending test specimens was doubled to provide extra flexural rigidity for meaningful tests.

The purpose of the testing program is to evaluate the elastic modulus of various FRP system configurations (E_I) using the direct tension specimens and to estimate the equivalent moment of inertia using the flexural testing specimens for each of the proposed configuration. Each specimen consisted of three FRP layers (Table 2).

Figures 4 and 5 show results for the stress-strain and load-deflection relation for typical specimens sets respectively. In general, three specimens were used for each set as laid out in Table 2.

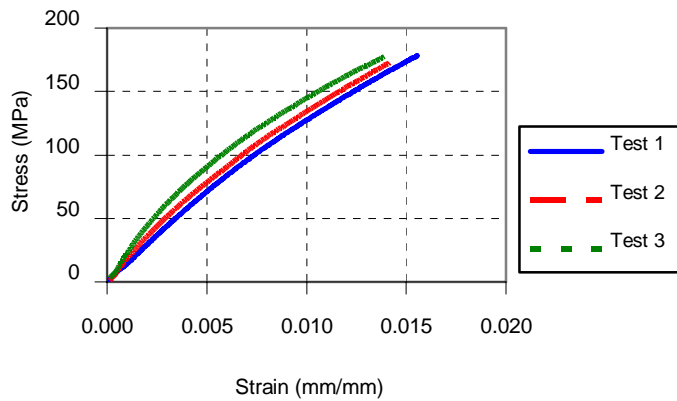
The flexural rigidity for specimens with the fiber architectures identical to those of the specimens used for the tensile tests was evaluated in the experiments. The purpose of the flexural tests is to establish a relationship between the applied load and the mid span deflection that results in experimental values for the stiffness ($E_I I$), where E_I is the elastic modulus along the beam direction and I is the sectional moment of inertia. The flexural tests were performed using two point loads at quarter distance from the supports.

The relationship between the mid-span deflection (Δ_{Max}) and the applied load (P) is given by

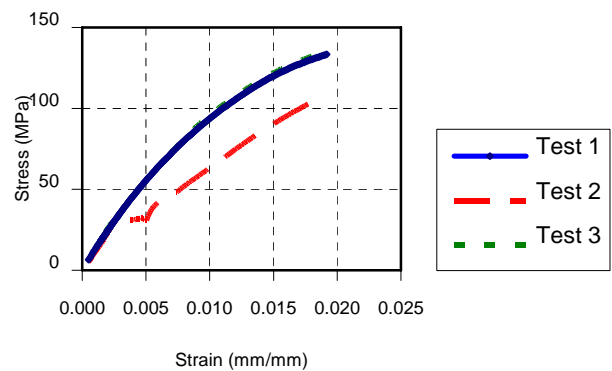
$$\Delta_{Max} = (2.75 \times P \times L^3) / (192 \times E_1 I) \quad (9)$$

Table 2. Testing Program for the various FRP Configurations
(a) Tensile Tests (b) Flexural Tests

Set No.	Outer Layers	Inner Layer	Size (mm)	Set No.	Outer Layers	Inner Layer	Size (mm)
1	0/90° Glass	±45° Glass	25.4×1.4×305	9	0/90° Glass	±45° Glass	25.4×2.8×203
2	0/90° Carbon	±45° Carbon	25.4×1.4×305	10	0/90° Carbon	±45° Carbon	25.4×2.8×203
3	0/90° Glass	±45° Carbon	25.4×1.4×305	11	0/90° Glass	±45° Carbon	25.4×2.8×203
4	0/90° Carbon	±45° Glass	25.4×1.4×305	12	0/90° Carbon	±45° Glass	25.4×2.8×203
5	±45° Glass	0/90° Carbon	25.4×1.4×305	13	±45° Glass	0/90° Carbon	25.4×2.8×305
6	±45° Carbon	0/90° Glass	25.4×1.4×305	14	±45° Carbon	0/90° Glass	25.4×2.8×305
7	±45° Glass	0/90° Glass	25.4×1.4×305	15	±45° Glass	0/90° Glass	25.4×2.8×305
8	±45° Carbon	0/90° Carbon	25.4×1.4×305	16	±45° Carbon	0/90° Carbon	25.4×2.8×305

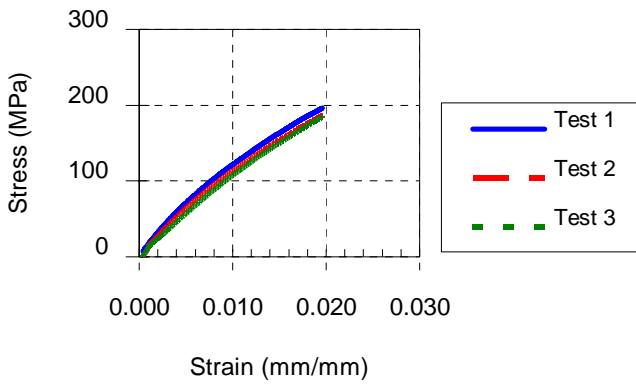


Set 1

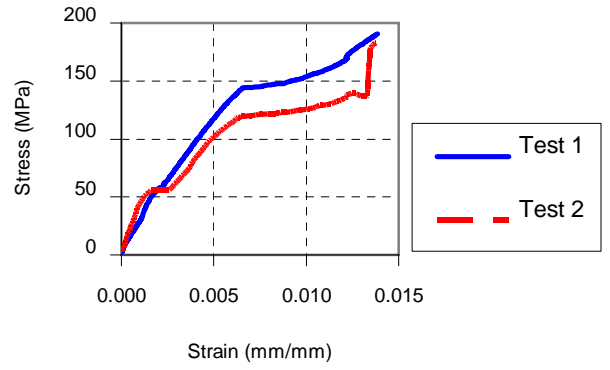


Set 3

Figure 4a: Typical stress-strain plots for sets

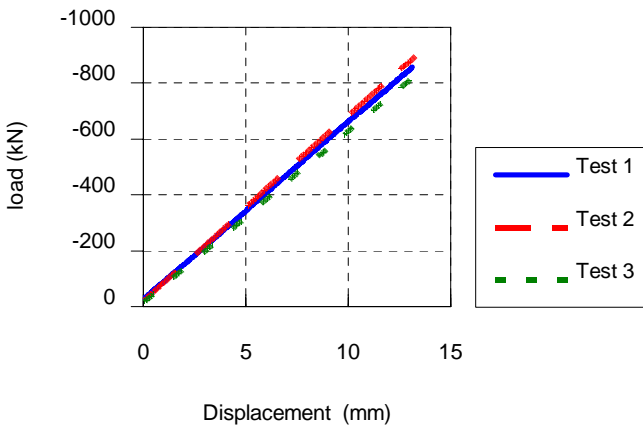


Set 6

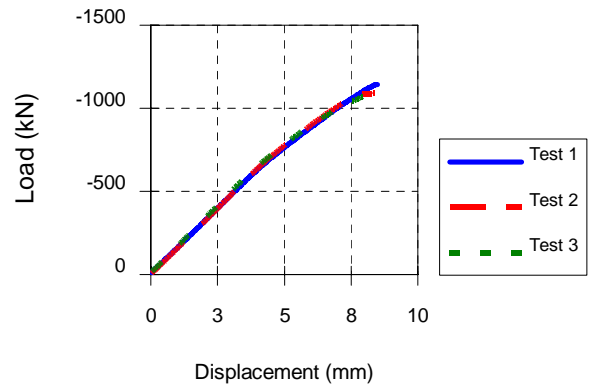


Set 8

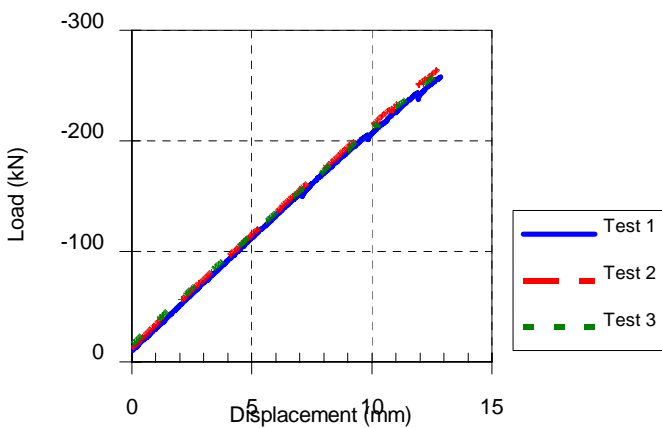
Figure 4b: Typical stress-strain plots for sets 6 and 8.



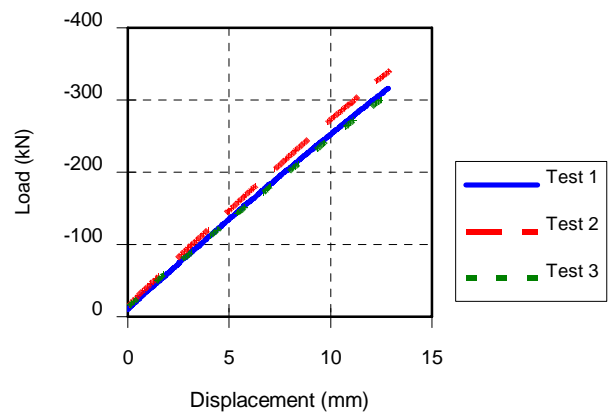
Set 9



Set 12



Set 13



Set 16

Figure 5: Typical load-deflection plots for sets 9, 12, 13 and 16.

Using Equation (9), an empirical relationship between the applied loads and mid span deflection was established. This relationship is based on the experimental results of load and mid-span deflection for sets 9 to 16, as can be seen in Figure 5.

4.2 Ductility Requirements

The ductility requirement was achieved by the out of the plane rigidity of the FRP retrofitting systems. The out of plane rigidity is required to confine the concrete of the connection core. The ACI 381-02 guidelines were used to provide the required rigidity. The equivalent rigidity was evaluated based on the assumption that, under the same lateral stress, the out of plane deflection of

the hoop steel is the same as the deflection of the retrofitting systems. The out of plane deflection of the steel was calculated based on the following analytical procedures.

Considering hoop steel with a spacing s between the hoops subjected to out of plane uniform stress q , the total linear load on one hoop is $(q \times s)$.

Based on the free body diagram in Figure 6, and with a moment at either end of the hoop steel, the following relationship between deflection and applied stress is established:

$$F \times Y = q \times s \times \left(\frac{L_h^2}{8}\right) \quad (10)$$

$$Y = q \times s \times \left(\frac{L_h^2}{8}\right) / (A_{sh} \times f_y) \quad (11)$$

Where, Y is the maximum deflection, F is the force in the hoop steel and L_h is the length of the hoop stirrup.

The bond stress between the hoop steel and concrete is ignored due to the symmetrical configuration of the hoop steel.

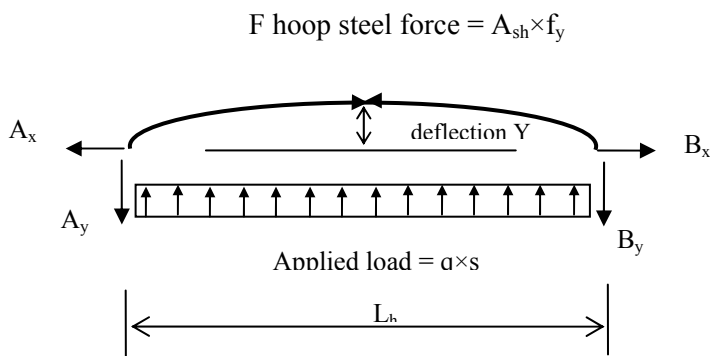


Figure 6: The free body diagram for a deflected hoop steel

In order for the replacement system to confine the concrete in the connection core, the maximum out of plane deflection should be limited to the value Y defined by Equation (11) under the same applied loads $(q \times s)$. This can be achieved if the right stiffness is designed for in the overlaying repair patch, as shown later. Considering the retrofitting system as a simply supported beam with a span equals to L_h . The maximum deflection under the $q \times s$ loads is:

$$Y = \frac{5}{384} \times \frac{q \times s \times L_h^4}{E_1 I}$$

Where, $E_1 I$ is the equivalent FRP stiffness over the spacing s .

Equating the deflection for both conditions, the stiffness $E_1 I$ is found to be as

$$E_1 I = \frac{5}{48} (L_h^2 \times A_{sh} \times f_y) \quad (12)$$

By incorporating the stiffness of Equation (12) with the experimental flexural tests results, keeping in mind that the FRP systems elastic modulus is determined from the direct tension tests, the stiffness for various FRP architectures and configurations can be evaluated.

Knowing the width of the FPR systems will be spread over the distance s (the steps between the hoop steel), Equation (12) can be used to determine the equivalent thickness of the FRP systems.

In this study, two FRP configurations are investigated:

The first system is assumed to be applied flat over the connection (constant thickness). The thickness is controlled by either the strength or ductility requirements. Table 3. Shows the results of obtaining the thickness based on the strength requirement (Equation 8) and the ductility requirement (Equation 12) for all 8 fibre architectures tested experimentally. It should be noted that Table 3 is calculated for the connection shown in Figure 2. The distance L_h is assumed to be 500 mm, while the steps between the hoop steel (s) is considered to be 100 mm. The hoop steel area (A_{sh}) is 3 legs of diameter 12 mm bars, that is 339 mm^2 . The yield stress on the hoop steel is 413.7 MPa.

The second FRP configuration consists of corrugated systems. The thickness of the system is determined by the thickness required for the strength requirements and the out of plane moment of iner-

tia is supplied by the stiffness provided by the corrugated shapes (see Table 4). The proposed corru-

gated shapes are shown in Figure 7 (a) and (b).

Table 3. The thickness of the overlay systems for various FRP architectures.

Set No.	Outer Layers	Inner Layer	Design stress f_{ul} (MPa)	Elastic Modulus E_1 (GPa)	Thickness Based on Strength* (mm)	Thickness Based on Ductility** (mm)
1,9	0/90° Glass	±45° Glass	172	17.2	16.3	29.7
2,10	0/90° Carbon	±45° Carbon	296	43.1	9.7	21.8
3,11	0/90° Glass	±45° Carbon	131	17.2	21.3	29.7
4,12	0/90° Carbon	±45° Glass	186	29.0	15.2	24.9
5,13	±45° Glass	0/90° Carbon	172	18.6	16.3	29.0
6,14	±45° Carbon	0/90° Glass	186	17.9	15.2	29.2
7,15	±45° Glass	0/90° Glass	152	14.5	18.8	31.5
8,16	±45° Carbon	0/90° Carbon	193	32.4	14.5	24.1

* Using equation 8

$$** [E_1 I / (E_1 \times s)]^{1/3} \text{ (where } E_1 I \text{ is calculated from eq. 12)}$$

The distance z is determined based on the ductility requirements. Attaching pre-fabricated FRP stripes to connection can ensure the corrugated shapes. The required z distance defines the thickness of the strips. The FRP will be lay-up on the top surface of the strips.

The circular shape shown in Figure 7 (b) is desirable for ensuring a continuous bond between the FRP systems and the concrete. Also, the use of circular shapes eliminates the difficulty of applying the FRP to the corners.

shown in Equation (12). For this system, the confinements requirements (stirrup spacing and cross sectional areas) as outlined in the ACI -318-02 must be used to find the thickness of the FRP overlays (Figure 8).

Table 4. Required thickness and step for various corrugated FRP architectures

Set No.	Outer Layers	Inner Layer	FRP Thickness (mm)	Step Z^* (mm)
1,9	0/90° Glass	±45° Glass	16.3	50.8
2,10	0/90° Carbon	±45° Carbon	9.7	45.7
3,11	0/90° Glass	±45° Carbon	21.3	48.3
4,12	0/90° Carbon	±45° Glass	15.2	44.5
5,13	±45° Glass	0/90° Carbon	16.3	43.2
6,14	±45° Carbon	0/90° Glass	15.2	44.5
7,15	±45° Glass	0/90° Glass	18.8	49.5
8,16	±45° Carbon	0/90° Carbon	14.5	33.0

* For a given thickness and E_1 values, z can be derived using the parallel line theory.

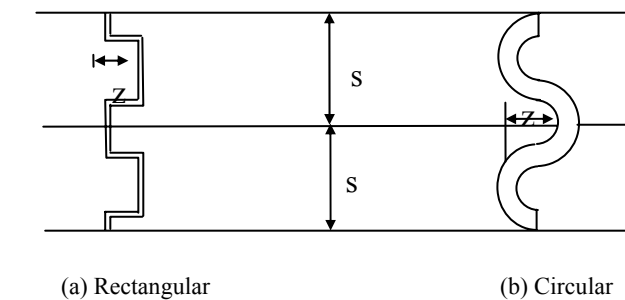


Figure 7: Proposed corrugated shapes for the FRP retrofitting systems

5 PROPOSED STRENGTHENING OVERLAYS

5.1 Type II joints

The following two systems were considered for Type II joints:

Multi-layered FRP system with two fibre layouts 1°, 90° and ±45°. The thickness of the system can be evaluated based on the ductility requirements as

Multi-layered corrugated FRP system with two fibre layouts 1°, 90° and ±45°. The thickness of the system will be evaluated based on the required equivalent strength (area of the stirrups) and depth coupled with the configuration of the corrugation will be established based on the confinement requirements (stirrup spacing),(Figure 9).

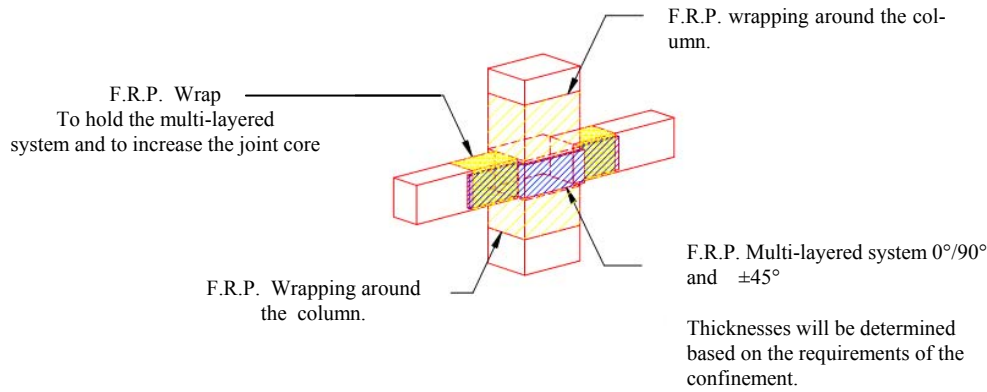


Figure 8: Multi-layered system for upgrading type II joints.

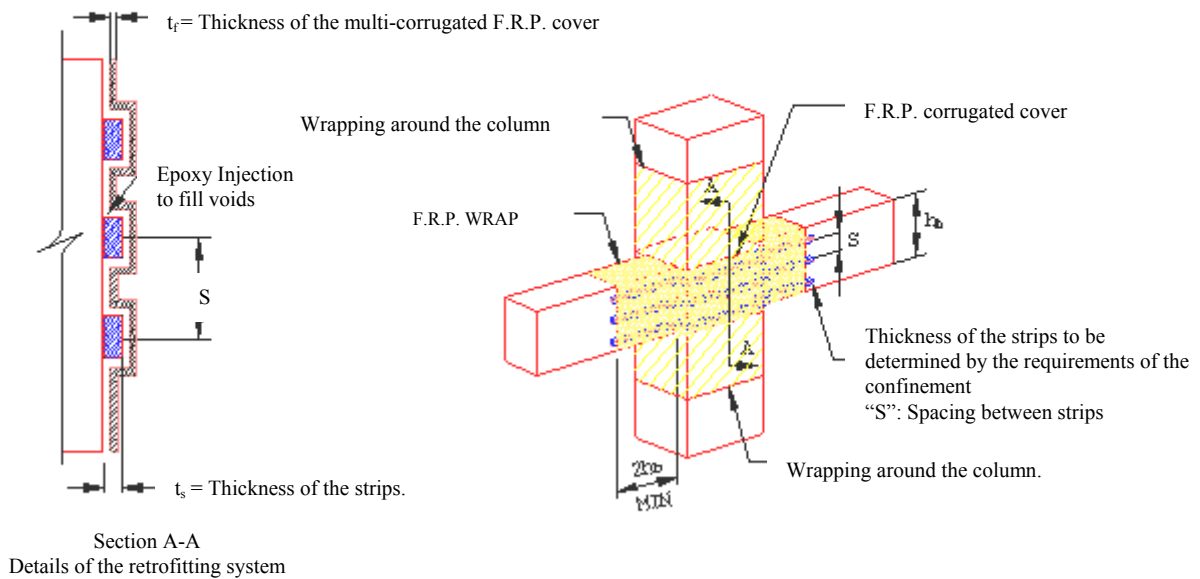


Figure 9: Multi-layered corrugated system for upgrading type II joints.

It is anticipated that the second system will result in a more efficient design. The ACI 318-02 Code requires the concrete of the joint core area to carry the applied shear force. Therefore, an attempt can be made to increase the core area by wrapping the connection beams to a new dimension that ensures sufficient core area to withstand the applied shear force

5.2 Type I joints

Type I joints also proposed to have two configurations.

Joints with insufficient confining spandrel beams and sufficient hoop steel. In this type of joints, FRP wrap will be constructed around the spandrel beams to satisfy the code requirements for considering the confinements due to the spandrel beams.

The requirement is specified as the $\frac{3}{4}$ of the connection face is covered by the cross-section of the spandrel beams, (Figure 10).

Joints with sufficient confining spandrel beams and insufficient hoop steel. In this type of joints, strips or rods are inserted through the spandrel beams after drilling holes as required to satisfy the transverse steel confinements. The rods or strips are epoxy injected and connected at the ends by wraps around the joint beams, (Figure 11).

Joints with insufficient confining spandrel beams and insufficient hoop steel. A combination of the above two systems will be investigated to upgrade the deficiencies of the connection.

The beams connecting the joints must be also investigated in terms of the core concrete area needed to provide the shear strength of the joints. In the case of any deficiency, beams wrapping may be required for increasing the core area.

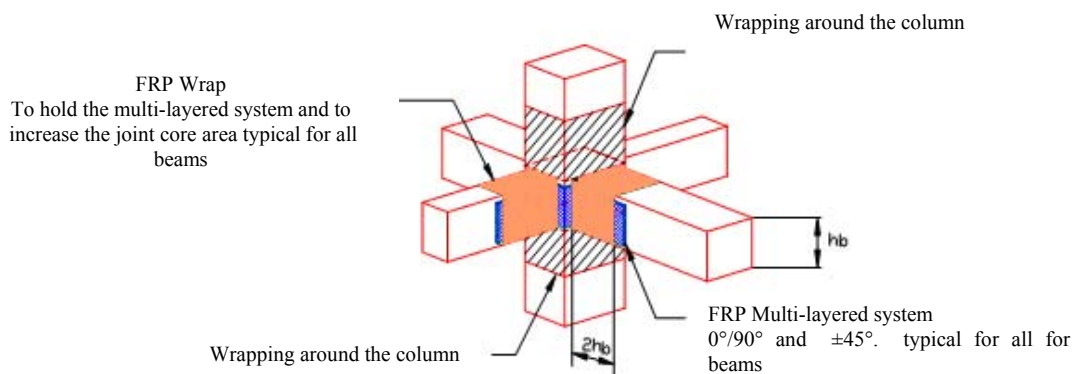


Figure 10: The multi-layered system for upgrading of type I joints with sufficient hoop steel.

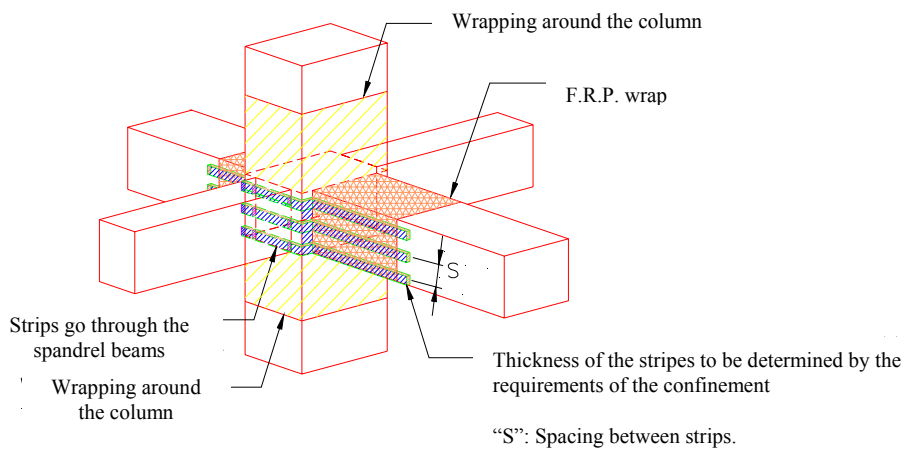


Figure 11: The multi-layered system for upgrading of type I joints with insufficient hoop steel.

In all of the above-recommended upgrades, both ends of the FRP systems must be rigidly fixed to beams to satisfy the fixed support conditions as-

sumed in the analysis. The end of the FRP support conditions can be ensured by either FRP-wrapping, mechanical fasteners or both.

6 CONCLUSIONS AND RECOMMENDATIONS

Based on the performed research investigation, the following recommendations can be concluded:

- The use of FRP systems is an effective method for upgrading deficient concrete connections to enhance the shear strength and ductility performance.
- Architecturally corrugated FRP retrofitting systems are an efficient option to provide out of plane rigidity for confining the concrete in the core of the connection. Corrugating of the overlays results in a reasonable thickness of the systems used.
- The combinations of $0/90^\circ$ and $\pm 45^\circ$ for the orientations of carbon fibres results in the least thickness of the FRP system. This combination can be implemented in the case where the option of architecturally corrugated FRP systems is obsolete.
- To ensure the ductility requirements, the ends of the FRP systems should be fixed to the beams forming the connection. This can be accomplished by wrapping of FRP materials around the FRP retrofitting systems.
- The developed work in this project is to be implemented in actual field applications. Therefore, more analytical analysis is needed to evaluate the elastic modulus of the laminated systems taking in consideration the fibre volumetric ratios and the layer thickness. This work is still in progress in North Carolina AandT Center of Composite Material Research.

7 ACKNOWLEDGEMENTS

This work could not have seen light without the support of North Carolina AandT Center of Composite Material Research. In particular, the authors wish to acknowledge the guidance of Prof. Naseer El-Haque whose devotion to academic excellence and unfailing support to his colleagues is a priceless treasure to all of us at Kuwait University.

8 REFERENCES

- ACI 318. 2002. Building Code Requirements for Structural Concrete (ACI 318-02) and Commentary (ACI 318R-02), American Concrete Institute.
- Bidda, A., Ghobarah, A. and T.S.Aziz, T.S. 1997. Upgrading of Non ductile Reinforced Concrete Frame Connection, Journal of structural engineering, ASCE, Vol. 123, No. 8. pp. 1001-1010.
- Gergely, J., Pantelides, C. and Reaveley, L. 2000. Shear Strength of RCT-Joints Using CFRP Composites, Journal for Composites for Construction, Vol. 4, No. 2, pp. 56-64.
- Hwang, S. and Lee, H. 1999. Analytical Model for Predicting Shear Strength of Exterior Reinforced Concrete Beam-Column Joints for Seismic Resistance, ACI, Structural Journal, Vol. 96, No. 5, pp. 846-857.
- Hwang, S. and Lee, H. 2000. Analytical Model for Predicting Shear Strength of Interior Reinforced Concrete Beam-Column Joints for Seismic Resistance, ACI, Structural Journal, Vol. 97, No. 1, pp. 35-44.
- Scott, R. H. 1996. Intrinsic Mechanism in Reinforced Concrete Beam-Column Connection Behavior, ACI Structural Journal, Vol. 93, No. 3, pp 336-346.
- Tsonos, A. G. 1999. Lateral Load Response of Strengthened Reinforced Concrete Beam-to-Column Joints, ACI, Structural Journal, Vol. 96, No. 1, pp. 46-56.